MATERIALE PLASTICE
https://revmaterialeplastice.ro
https://doi.org/10.37358/Mat.Plast.1964

Starch Modified Tough Biocompatible Polyurethane/acrylamide bio Composites: Physicochemical Properties and Biodegradation Studies

JEEVITHA VEDAIYAN[1], RAVICHANDRAN KANDASWAMY[2]*, LYNDA MERLIN DASAIEN[3]

[1]Department of Chemistry, Anna University, Madras Institute of Technology, Chennai 600044, Tamil Nadu, India
[2]Department of Rubber and Plastics Technology, Anna University, Madras Institute of Technology, Chennai 600044, Tamil Nadu, India
[3]Department of Chemistry, University College of Engineering, Arni 632326, Tamil Nadu, India

Abstract: *Biodegradable bio composites with potential applications in medical implants were prepared with starch content by in situ polymerization technique using polyurethane prepolymers. (PU) and acrylamide (AAM) monomers. The structure and properties of bio composites were evaluated. FT-IR spectroscopy showed bonding between N=C=O functional group terminated polyurethanes confirmed improved compatibility of prepolymers, AAM, starch and bio composites. The DSC data are the glass transition (Tg) of the bio composite and ordinary polyacrylamide (PAAM) network. By incorporating starch and polyurethane in the form of an interpenetrating network into a polyacrylamide network, mechanical and thermal properties of bio composites due to higher crosslink density given by hard segment content. We studied the swelling behavior of both bio composites and individual PAAM networks under different pH conditions to validate their biocompatibility and potential use in biomedicine setting. The hydrolytic stability of biocomposites and PAAM networks was investigated using phosphate buffer. Hydrolytic stability of biocomposites was found to be higher comparison with PAAM network. Morphological analysis of the samples showed uniform distribution and good interfacial adhesion. Improves sample biodegradability it was revealed by the soil runoff test.*

Keywords: *A. Biocomposites, B. Mechanical properties, B. Thermal properties D.SEM Analysis, Swelling behaviours*

1. Introduction

Bio composite polymers are composed of one or more biobased components. Due to its excellent properties such as light weight, low density, and low electrical and thermal conductivity, high corrosion resistance and improved mechanical properties Polyurethane-based bio composites are attracting attention in various fields [1, 2]. Polyurethane has proven to be a potential material.

Their high mechanical strength, flexibility, fatigue resistance, and biocompatibility make them suitable for biomedical applications [3-5]. In recent years, research has focused on this development of a modified system exhibiting improved miscibility. Polymer compatibility can be improved by establishing physical and/or chemical interactions between polymers component. One approach to this is to link polymers in the form of interpenetrating polymer networks (IPNs). B. Crosslinking, Interchain Entanglement, and Finally Crosslinking Grafting [6,7]. IPNs may help improve the mechanical strength and elasticity of polymers compared to single ones due to physical entanglement and network interactions networked networks [8,9].

Synthetic hydrogels such as PHEMA and PAAM are hydrophilic materials of great interest. This is because these polymers can absorb large amounts of water within their structure, swell, and retain large amounts of water. [10-11]. Due to its excellent water absorption properties, this kind of biomaterial is used in various biomedical applications such as: B. Controlled drug delivery, tissue, very promising Engineering material, wound healing, etc. [12]. The ability of hydrogels to absorb water derives from

email: ravi@mitindia.edu

the hydrophilic functional groups attached to the polymer backbone, whereas the resistance to dissolution derives from this. Interconnections between network chains [13]. However, the mechanical properties of swollen polyacrylamide gels are generally poor and reinforcement is often desired or the mechanical strength of polyacrylamide gels was improved by incorporating 10% polyurethane in the form of an interpenetrating polymer network [14, 15]. Therefore, hydrogels in the form of bio composites are mandatory. Synthesis of biodegradable polymers from environmentally friendly materials has increased research interest in waste treatment with degradable conventional plastics [16]. This process is very expensive and growing interest in this topic has led to the development of low-cost biodegradable thermoplastics. One of the technologies that produce biodegradability thermoplastics are made by adding units containing functional groups, such as starch, which promote the decomposition of thermoplastics [17]. Research continues on the development of Low-density biodegradable polymers by physically blending natural renewable polysaccharides such as starch, cellulose and chitosan with the polymer to promote microbial attack [18, 19]. Under Starch, a natural biopolymer, has received much attention due to its renewable nature, biodegradability, low cost, and abundant abundance [20]. In addition, it is moisture sensitive and brittle. Thermoplastic starch limits its possible uses [21].

Various studies on starch-based blends and composites have shown poor mechanical properties due to the incompatibility of starch and polymer and have not been widely used. Especially as a biomaterial. The lowest compatibility is due to the non-polar or polar character of hydrophobic polymers or hydrophilic starches [22, 23]. Starch, chitosan, cellulose, lignin and chitin are used as additives in bio composites to improve the mechanical and thermal properties of polymer matrices and inherit all the advantages of natural polymers [24-26]. Compatibilizers such as N=C=O functional group (NCO) - terminated polyurethane prepolymers are incorporated into starch-based bio composites to improve their compatibility. Improve interfacial adhesion between Starch and prepolymers, in turn, improve the mechanical and thermal properties of bio composites.

The swelling rate of bio composites depends on their network structure. It is monitored by the state of cross-linking polymerization or by incorporating more hydrophilic comonomers into the network structure [27-30]. This research carried with development of sustainable and biocompatible bio composites using starch-modified polyurethane-acrylamide networks. Fourier transform infrared (FTIR) spectroscopy, thermal expansion, bio composite properties, SEM analysis, mechanical and biodegradability studies were investigated. As a result, the mechanical and thermal properties of starch are improved. Bio composites incorporating polyurethane compared to individual polyacrylamide networks (PAAM), addition of starch improves hydrolytic stability with NCO-terminated polyurethane prepolymers within a polyacrylamide network. Biodegradation tests are carried out by the burial method. The degree of biodegradation of the sample is assessed with Weight loss rate, Sample degradation may be due to hydrophilic secondary features present.

2. Materials and methods

2.1. Materials

Polytetramethyleneetherglycol (PTMEG) polyols based on a tetramethylene ether backbone with a molecular weight of 1000 and a viscosity of 1000-2000 cps (70°C) were obtained from BASF as commercial grade chemicals. The polyol was degassed at 70°C for 3 h. Modified polymeric 4,4'-diphenylmethane diisocyanate (MDI) or polymeric MDI™ (commercially known as Rubinate 9433) was used as received from Huntsman. This material has an isocyanate equivalent weight of 132 and a free N=C=O functional group content of 31.09%. It was stored at 15-25°C under a nitrogen atmosphere before use. Benzoyl peroxide (BPO) is 1:1 Using a mixture of methanol and chloroform. Dibutyltin dilaurate (DBTDL) (MERCK) was used as catalyst for urethane reactions without further purification. Acrylamide (AAM) was purified by recrystallization from benzene. mp 84-85°C. Sodium chloride, sodium hydroxide, N,N'-methylenebisacrylamide (MBAAM), potassium persulfate, 2-bromophenol B, hydrochloric acid, sulfuric acid, etc. used in this study were all of analytical grade and were further

purified. I used it as is. Sago starch was sourced from a local market and used without further pre-treatment.

2.2. Fabrication of Biocomposite Samples

2.2.1. Preparation of Polyacrylamide Hydrogel (PAAM)

Acrylamide monomer (AAM) (1 g) and N, N'-methylenebisacrylamide (MBAAM) (1%) were dissolved in 2 mL deionized water. A 1% potassium persulfate solution (2 mL) was added and the solution was purged with nitrogen for 15 min to remove dissolved oxygen. Polymerization was carried out in a constant temperature bath at 55°C for 30 min. The resulting crosslinked polyacrylamide gel was washed with distilled water and the gel was soaked in deionized water for 24 h to remove unreacted monomers and residual initiator. The yield of crosslinked gel was calculated as 96% by measuring initial and final weight of the polyacrylamide hydrogel.

2.2.2. Preparation of Starch Incorporated Polyacrylamide-based Hydrogels (PAAMSS)

Acrylamide monomer (AAM) (1 g) and N, N'-methylenebisacrylamide (MBAAM) (1%) and 2% starch by weight relative to acrylamide monomer were mixed with 2 mL of deionized water and 2 mL of 1% sulfuric acid peroxide dissolved in potassium solution were added. The solution was purged with nitrogen for 15 min to remove dissolved oxygen. Polymerization was carried out in a constant temperature bath at 55°C for 30 min. The resulting crosslinked starch-grafted polyacrylamide gel was washed with distilled water and the gel was soaked in deionized water for 24 h to remove unreacted monomers and residual initiator. The yield of crosslinked gel was 97%.

2.2.3. Preparation of NCO–Terminated Polyurethane Prepolymer (PU)

For the preparation of the NCO-terminated polyurethane prepolymers, the modified polymer MDI with various NCO/OH ratios and polytetramethyleneether glycol (PTMEG) polyol of 1000 molecular weight was mixed slowly with stirring using a mechanical stirrer and a very large stirrer. added to the three-necked flask provided. A small amount of added catalyst DBTDL was added, 1,4-butanediol (BDO) was added for chain extension, and the mixture was reacted at 90°C to 100°C for 3 h while purging with nitrogen gas. When the isocyanate group content of the reaction mixture reached the theoretical value, the end of the reaction and disappearance of the monomer was determined by di-n-butylamine titration. This was also confirmed by the characteristic absorption peak at 2270 cm^{-1} of the NCO group.

2.2.4. Preparation of Starch Incorporated Polyurethane Polyacrylamide Based bio Composite (PU/PAAM/SS)

Bio composites were fabricated in two steps. In the first step, we prepared an NCO-terminated polyurethane prepolymer based on his PTMEG polyol with a molecular weight of 1000. In the second stage, a polyurethane prepolymer, acrylamide monomer (AAM), N, N'-methylenebisacrylamide (MBAAM) (0.01% w), BPO (0.5% w/w), and different weight percentages of starch (2% and 5% on polyurethane prepolymer) and acrylamide monomer dissolved in 2 mL of THF solvent, 0.1% TEA and 2 mL of 1% potassium persulfate solution were added. The mixture was stirred at room temperature for 15 min to form a homogeneous solution. The temperature was then raised to 70°C to initiate polymerization of acrylamide. After stirring for 1 h, the viscous solution was degassed to remove trapped air bubbles, poured into glass molds and kept in a preheated oven maintained at 60°C. It was held at this temperature for 24 h and at 100°C for 2 h to promote complete network formation. The film so formed was slowly cooled, removed from the mold and the dried sample was used for further testing.

2.3. Characterization Techniques

2.3.1. FTIR Spectroscopy Analysis

Fourier Transform Infrared (FTIR) spectra were obtained in the 4000-400 cm^{-1} wavenumber range for all composite samples using KBr pellets on a Spectrum One FTIR (Perkin-Elmer Instruments, USA).

2.3.2. Thermogravimetric Analysis (TGA)

Thermogravimetric analysis (TGA) was performed (15miligram sample mass) on a thermal analyzer STA 409PC from NETZSCH-Geratebau GmbH(10 - 20 mg is sufficient for most applications)at a temperature range from room temperature to 900°C in presence of nitrogen atmosphere with a usual heating rate for polymers (20°C per min). 10°C/min - 20°C/min are typical rates are followed. It is important to determine approximate mass and the rate most appropriate for the material. Powders samples are ideal because we can maximize surface area which can improve resolution.

2.3.3 Differential scanning calorimetry (DSC)

Differential scanning calorimetry (DSC) thermograms were obtained for 50 miligram sample mass using a DSC 200PC thermal analyzer (NETZSCH-Gerätebau GmbH) in the 2nd run of DSC scan. The heating rate was 20°C min^{-1} in the temperature range from -150°C to 300°C.

2.3.4 Water Absorption Study

Water absorption of PAAM and bio composite samples was measured by immersing sliced PAAM and bio composite membranes in a beaker of water at 37°C. The 1 mm thick membrane was cut into circular discs with a diameter of 20 mm using a sharp stainless-steel knife. Samples were weighed every 10 min until the maximum moisture content was reached. The equilibrium water content (EWC) was calculated according to the following formula:

$$EWC(\%)=[(WS-Wd)/Wd]\times 100$$

where WS and Wd are the weights of water absorbed and dry sample, respectively.

2.3.5. Hydrolytic Stability

Hydrolytic stability was determined as follows: Twelve pre-weighed dry samples were saturated with phosphate buffer (*p*H 7.4), stored in sealed glass vials, and stored in an oven at 80°C. After 3, 5, 7, and 14 days he took 3 samples. They were washed with distilled water and dried at 80°C for 16 h. The percent weight loss of samples after different test periods was obtained by comparing the weight of dry samples before and after testing.

2.3.6. Tensile Strength and Elongation

The tensile strength and elongation of the samples were measured with a universal testing machine at a crosshead speed of 5 mm min^{-1}. Both dried and swollen samples were measured. Tensile specimens 1 mm thick and 6 mm wide were cut from the sheets.

2.3.7. Scanning Electron Microscopy (SEM)

Phase morphology was examined with a Leo Stereo Scan 440 scanning electron microscope. Samples were ground in liquid nitrogen to maintain sample morphology and sputter-coated with gold prior to microscopic observation

2.3.8. Biodegradation Studies

A number of factors determine the rate at which this degradation of organic compounds occurs. Factors include temperature, humidity, types of soil, microbial charge etc., The degradation rate of many organic compounds is limited by their bioavailability, which is the rate at which a substance is absorbed

into a system or made available at the site of physiological activity as compounds must be released into solution before organisms can degrade them. The rate of biodegradation can be measured in a number of ways. In our study, the biodegradability of bio composites incorporating starch was investigated by soil burial test. Biodegradable bio composites offer the unique advantage of degrading in an aqueous environment, eliminating the need for post-use removal. A soil burial test is a biodegradation test performed in agricultural soil under normal conditions (Day temperature ranges from 81°F to 83°F, night temperature ranges from 89°F *to* 91°F, average humidity – 69%). The bio composite (1 g weight) was buried in the ground at a depth of 30 cm. Samples were taken from the soil at regular intervals of 7 days. The samples were washed with distilled water and dried in a vacuum oven at 40°C to constant weight [31]. The percentage of decomposition was calculated using the following formula:

$$\text{Biodegradation rate (\%)} = (Wi\text{-}Wf)\ /Wi \times 100$$

where Wi is the initial weight of the hydrogel and Wf is the final weight after 7 days.

3. Results and discussions

3.1. FT-IR Analysis

The FTIR spectra of samples (a) PAAM, (b) pure sago starch and PAAMSS, (c) PU and PU/PAAM, (d) PU/PAAM/SS are shown in Figure 1. Spectrum (a) shows a typical structure of a polyacrylamide (PAAM) network. The strong absorption at 3435 cm^{-1} and the composite peak at ~3200 cm^{-1} are due to N-H stretching of primary amides. Crosslinked polyacrylamide exhibits characteristic absorption peaks at 1655–1665 cm^{-1} (strong), 1618 cm^{-1} (weak), and 1352 cm^{-1} (weak) for C=O, N-H bending, and C-N stretching, respectively. indicates of the CONH Group. FTIR spectra b of pure starch and starch-grafted polyacrylamide (PAAMS) networks both show that the glucoside rings of starch are between 3700 cm^{-1} and 3200 cm^{-1} and between 1160 cm^{-1} and 1030 cm^{-1}. shown to have corresponding broad absorption bands. 1 is characteristic. In addition, there are differences in the intensity of this band for starch-grafted acrylamide samples due to the starch hydroxyl groups used. A strong absorption peak at 1675 cm^{-1} corresponds to the presence of CONH groups.

FTIR spectra of NCO-terminated polyurethane prepolymer (PU) and polyurethane-incorporated polyacrylamide-based polymer (PU/PAAM) are shown in Figure 1c. The FTIR spectrum of the polyurethane prepolymer showed characteristic absorption bands at 1728 cm^{-1} and 3298 cm^{-1} corresponding to the C=O groups of the urethane linkage and the N-H stretch of the urethane amide. Since the prepolymer is isocyanate-terminated, a strong and sharp absorption band due to NCO groups was observed at 2272 cm^{-1}. The FTIR spectrum of the PU/PAAM polymer showed no characteristic absorption band at 2270 cm^{-1}, confirming the grafting and interpenetration of acrylamide with the NCO-terminated polyurethane prepolymer. The peaks around 1630-1650 cm^{-1} and faint bands around 1292-1330 cm^{-1} correspond to C=O, N-H bending and C-N stretching of CONH groups in polyacrylamide. The peaks around 1510-1633 cm^{-1} may be due to urea groups formed by reaction of acrylamide monomers with polyurethane prepolymer.

The FTIR spectrum of a polyacrylamide-based bio composite (PU/PAAM/SS) made of starch and polyurethane is shown in Figure 1d. There is a band at 3302 cm^{-1}, which can be attributed to the bound NH band of the polyurethane above the broad OH band. A carbonyl band bound at 1723 cm^{-1} corresponds to the structure of starch interfaces with polyurethane can also be observed. These two bands also confirm the grafting between the starch and polyurethane phases. Thus, it was confirmed that the OH groups of acrylamide monomers and starch reacted with the NCO groups of PU [21].

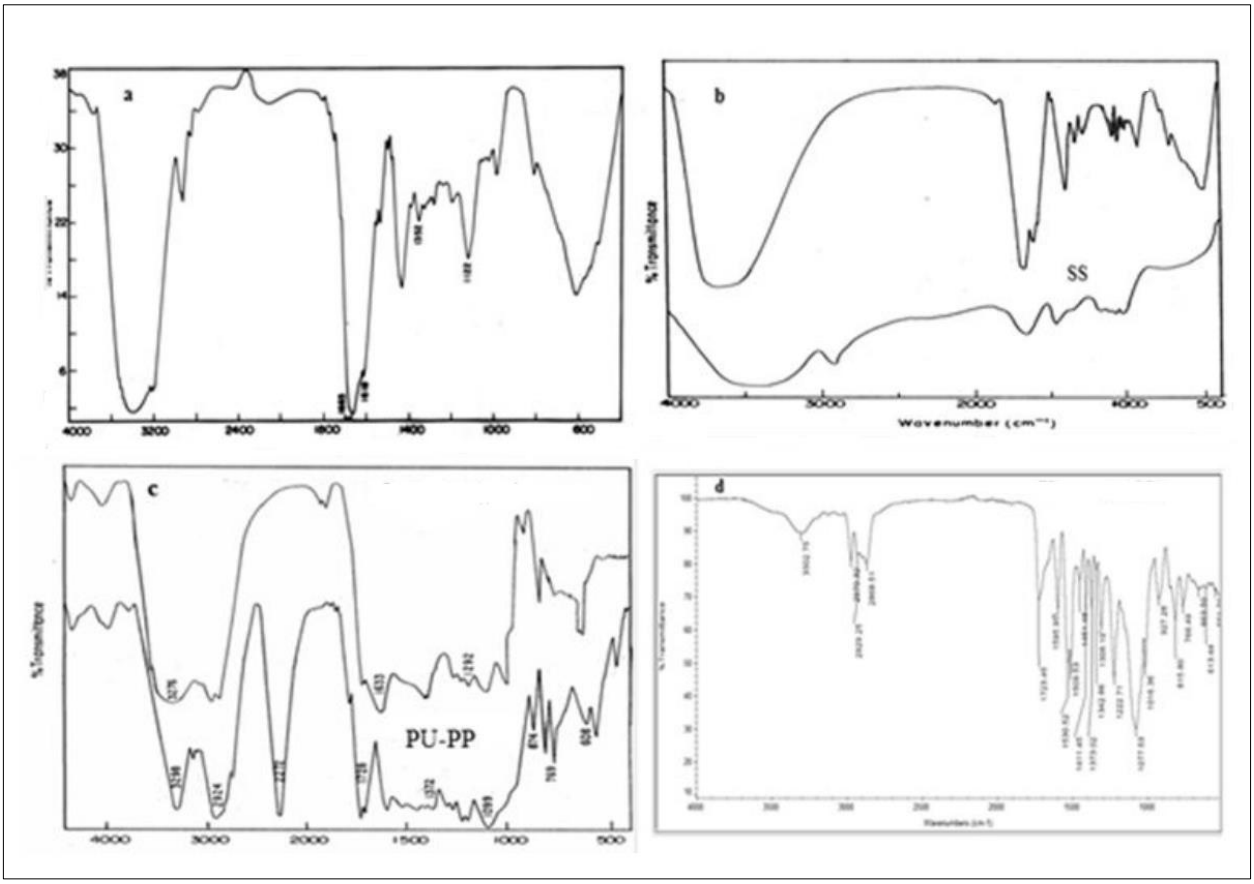

Figure 1. FTIR spectra of samples (a) PAAM, (b) Pure sago starch and PAAMSS, (c) PU and PU/PAAM (d) PU/PAAM/SS. The spectra show that the interactions between PU, AAM and SS contents are evidenced and the structure of biocomposite is characterized

3.2. Thermal Behaviour of the Biocomposites

TG thermograms of PAAM (a), pure sago starch (b), PAAMS (c), PTEMU-PP (d) and PTEMU-PP/PAAM/S (d) samples are shown in Figure 2. As shown in Figure 2a, the mass loss above 210°C was attributed to degradation of the PAAM network due to the loss of ammonia through the formation of imide groups upon cyclization [32]. Decomposition of volatile products such as water and ammonia has been observed below 320°C. Decomposition of the cyclized product was observed from 381°C. The TG thermogram of the PAAM network shows three stages of decomposition with maximum mass loss at 381°C. As shown in Figure 2b, the TGA thermogram of pure sago starch showed two stages of degradation with maximum mass loss at 316°C. Initial mass loss is due to the presence of water. The starch decomposition temperature in the second stage was found to be about 278-318°C. This may be due to the dissociation of glycosidic bonds. As shown in Figure 2c, the TG thermogram of the PAAMSS network showed three stages of decomposition with maximum mass loss at 390°C. Degradation of glucoside starch bonds were observed from 240°C. As shown in Figure 2d, the TG thermogram of the PU/PAAM network showed a maximum decomposition in the temperature range of 250-450°C

TG thermograms of PU/PAAM/SS are shown in Figure 2e. From thermal analysis, the bio composites were observed to exhibit two stages of decomposition. The first stage of degradation was due to the breakdown of glycosidic bonds in starch. A second stage of degradation may be due to dehumidification of the network structure. The bio composite PU/PAAM/SS showed maximum decomposition in the temperature range of 490-590°C, while PAAM showed maximum decomposition in the temperature range of 284-314°C. This indicates that the bio composites incorporating PU and starch are more stable compared to the PAAM network. This may be due to more effective interpenetration and tighter packing of molecular chains, which enhances thermal stability. TGA

thermogram data for pure sago starch, PAAM, PAAMSS, PU/PAAM, and PU/PAAM/SS are shown in (Table 1).

Table 1TGA thermogram data for PAAM, PAAMSS, PU/PAAM and PU/PAAM/SS Samples

Sample code	Stages of decomposition		
	I	II	III
Pure starch	105°C	278-318°C	-
PAAM	180-210°C	284-314°C	381- 425°C
PAAMSS	115-195°C	240-380°C	390- 450°C
PU/PAAM	120-257°C	250-450°C	-
PU/PAAM/SS	250-380°C	490-590°C	-

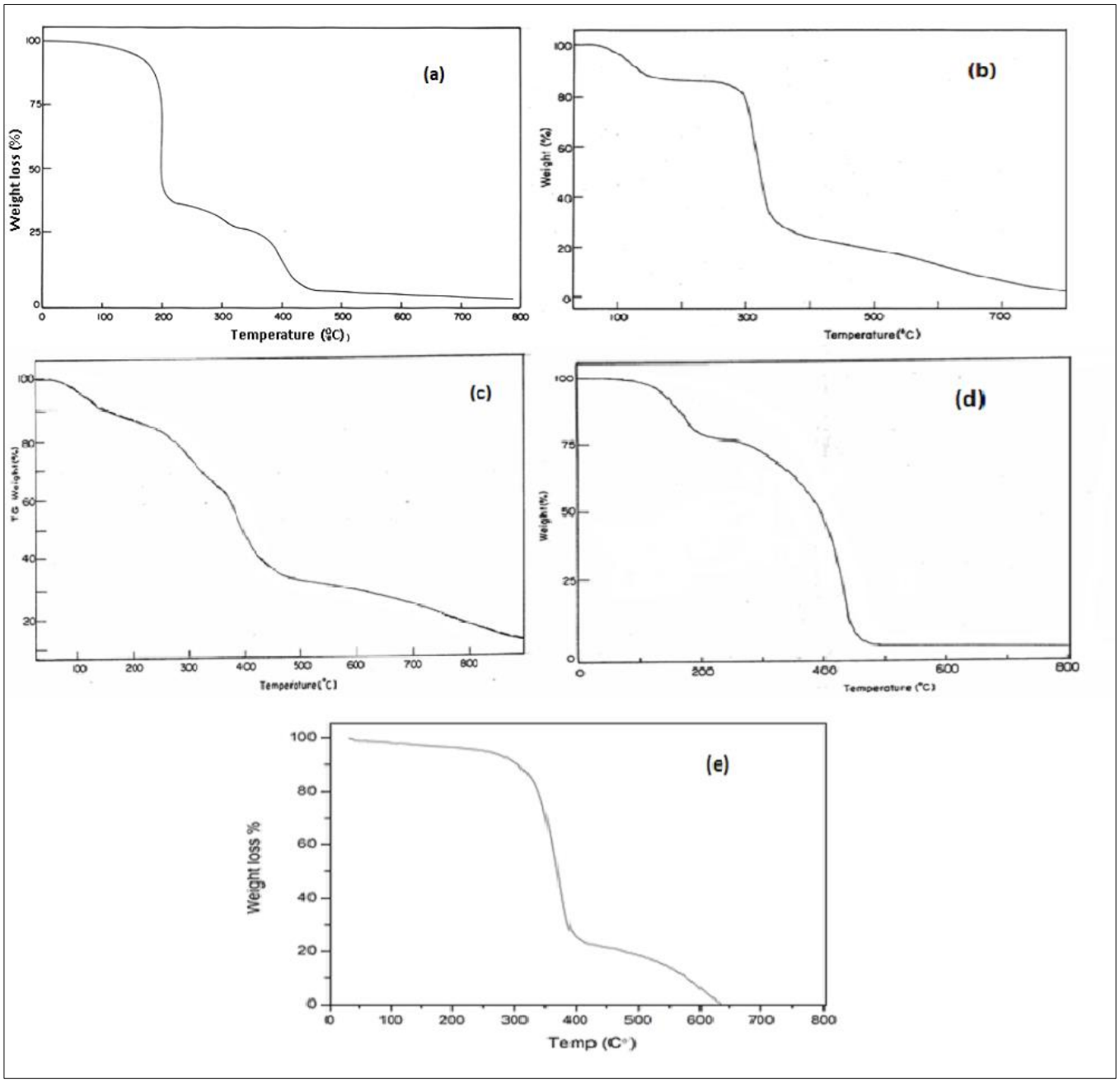

Figure 2. TGA thermogram of a sample PAAM (a), Pure sago starch (b), PAAMSS(c), PU/PAAM (d) and PU/PAAM/SS (e). The thermogram show that the interactions between PU, AAM and SS contents are evidenced and the enhanced thermal stability of the biocomposite is observed. More detailed data are in Table 1

3.3. Phase transition Temperature Analysis

Figure 3a PAAM DSC thermograms of PAAM (a), pure sago starch (b), PAAMSS (c), PU/PAAM (d) and PU/PAAM/SS (e) samples. A DSC thermogram of the network showed a single glass transition temperature (Tg) in the range of 75-80°C and an endothermic peak at 110°C due to the melting of the PAAM network. DSC thermograms (Figures 3b and 3c) of pure sago starch and PAAMSS samples showed a single glass transition temperature. Glass transition temperatures (Tg) (Table 2) of 60–80°C and 92-93°C were observed in the DSC thermograms of pure sago starch and PAAMSS samples, respectively. The Tg of PAAMSS is higher than that of PAAM networks. This was due to a shift in the Tg of PAAMSS to higher temperatures compared to that of PAAM, resulting in decreased chain mobility due to increased crosslink density, confirming the grafting of starch onto acrylamide monomers by crosslinks [33]. The DSC thermogram of the PU/PAAM sample (Figure 3d) showed overlapping Tgs based on the inflection points corresponding to those of PU (lower) and PAAM (higher). As shown in Figure 3e, the thermograms of PU/PAAM/SS exhibit a single glass transition temperature (Tg) in the range of 90-100°C, with an exothermic peak at 196°C for PAAM starch. It is due to crystallinity content. The transition temperature of the PU/PAAM/SS biocomposites is higher, probably due to the increased crosslink density within the network and the crystallinity of the acrylamide monomers and starch.

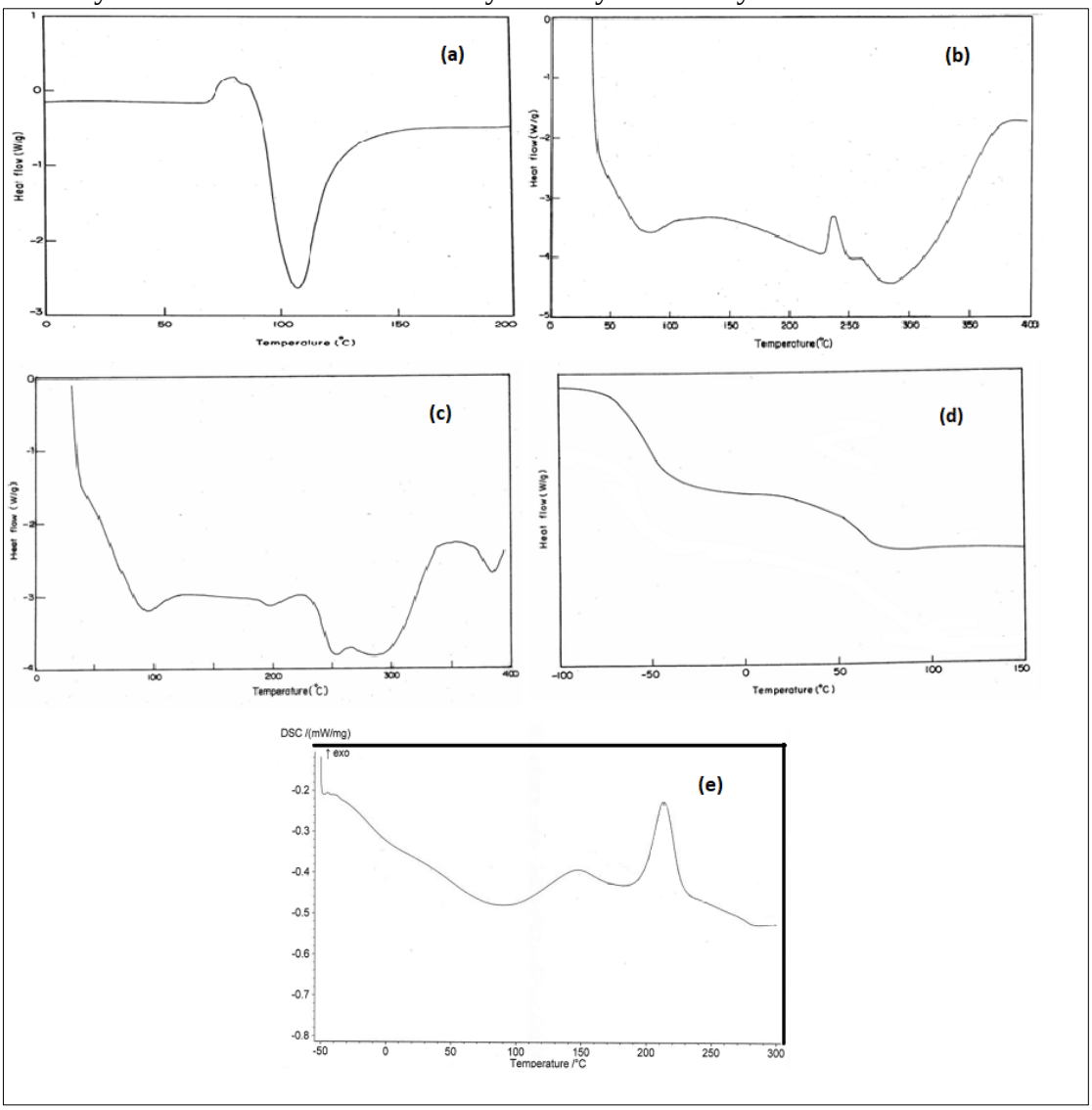

Figure 3. DSC curves of a Sample PAAM (a), Pure sago starch (b), PAAMSS (c), PU/PAAM (d) and PU/PAAM/SS (e). The transition temperatures show that the interactions between PU, AAM and SS contents are evidenced and the transition temperature of biocomposite is higher due to incorporated starch content. More detailed data are in Table 2

Table 2. DSC thermogram data for PAAM, PAAMSS, PU/PAAM and PU/PAAM/SS Samples

Sample code	T_g
PAAM	75-80 °C
Pure starch	60-80°C
PAAMSS	92-93°C
PU/PAAM	- 43°C, 66.2°C
PU/PAAM/SS	90-100°C

3.4. Swelling Studies

A PAAM network was created from 1% of the crosslinking medium MBAAM. Table 3 shows equilibrium swelling ratios of PAAM and PAAMSS networks of 406% and 1784% respectively. We found that the equilibrium swell ratio of the PAAMSS network is higher than that of PAAM. This may be due to the increased hydrophilicity of the network caused by starch incorporation into acrylamide hydrogels. The source data for the PU/PAAM/SS biocomposites are shown in Table 3. We found that the swelling behavior of the biocomposite was reduced compared to the PAAM network. This may be due to the increased crosslink density of the PU/PAAM/SS bio-composites and network interpenetration, which caused the network to become less flexible. This makes it difficult for water to be absorbed inside the net structure. Another reason for the observed decrease in swelling ratio is that increasing hydrophilic segments in the network decrease the volume fraction of the polymer and decrease the free volume mesh size. Apparently, decreasing the mesh size allows fewer water molecules to enter the network.

The effect of *p*H in modulating water sorption of polymer networks is more important. This is because changing the *p*H of the swelling medium often changes the free volume accessible to invading water molecules, which affects the swelling properties of the network. In this study, both acidic *p*H 4 and basic *p*H 9 were performed and the results are shown in Table 3. Equilibrium swelling was found to increase at *p*H 9 but decrease at *p*H 4 for PAAM, PAAMSS, and PU/. PAAM/SS. This is because acrylamide undergoes partial hydrolysis as *p*H increases, creating anionically charged centers along the copolymer chains, causing repulsion between polymer chains, expanding the free volume within the network, and increasing water absorption. This is due to the fact that it increases the rate.

3.5. Hydrolytic Stability

Hydrolytic stability is an important property in determining the stability of biocomposites for use in medical devices. The presence of amide groups in the PAAM network makes it susceptible to hydrolysis in acidic and basic media. In the PAAM network, the presence of the network structure enhanced the hydrolytic stability due to cross-linking. Hydrolytic stability was evidenced by the mass loss and moisture content change of the dry samples. A mass loss of 5% or less over 14 days was considered stable in medical devices such as a contact lens (34). The hydrolytic stability of all PAAM, PAAMSS, and PU/PAAM/SS hydrogels in the network (Table 3) showed less than 5% mass loss over 14 days, indicating sample leaching and reduced stability of the hydrogel, Network stability is due to crosslink density. For PAAM and PAAMSS, network hydrolysis increased with increasing basal medium, whereas for PU/PAAM/SS biocomposites, increasing cross-linking decreased hydrolysis, thereby increasing the mass loss rate also decreased. This clearly demonstrates the stability of the biocomposite compared to individual PAAM networks.

Table 3. Swelling and Hydrolytic stability data for PAAM, PAAMS and PU/PAAM/SS

Sample code	Equilibrium Swelling Ratio (%) at different *p*H			% mass loss			
	7	4	9	3 Days	5 Days	7 Days	14 Days
PAAM	406	352	412	0.41	0.64	0.73	0.82
PAAMSS	1784	937	1092	0.59	0.61	0.64	0.71
PU/PAAM/SS	360	362	402	0.40	0.58	0.61	0.64

3.6. Mechanical Properties

Tensile Strength and Elongation

Tensile strength and elongation data for all samples PAAM, PAAMSS and PU/PAAM/SS are shown in Table 4. Significant increases in tensile strength and elongation were observed for both PAAMSS and PU/PAAM/SS meshes. Comparison with PAAM network. Incorporating polyurethane prepolymer and starch into AAM monomer improved the tensile and elongation properties of PU/PAAM/SS biocomposites. The 20/80 ratio (mole %) showed improved tensile and elongation properties, while the other compositions showed phase incompatibility. The presence of NCO/OH content in the polyurethane prepolymer and starch increases the tensile strength of the biocomposite. This may be due to the higher crosslink density mediated by the hard segment content and network interpenetration [35]. The biocomposite PU/PAAM/SS exhibited higher elongation properties compared to PAAM and PAAMSS. This may be due to the high flexibility conferred by the low molecular weight PTMEG soft segment. The tensile strength of the swollen network was lower compared to the dry gel because water molecules entrapped in the network reduced the tensile strength of the network. This phenomenon was reversed for the elongation of PU/PAAM/SS biocomposites. This is because the interpenetration of the network structure reduces the sustained water uptake within the network, thus enhancing elongation in the swollen state. The highest mechanical strength of biocomposites is due to the chain distribution and molecular non-covalent interactions resulting from the entanglement of the network structure.

Table 4. Mechanical studies data for PAAM, PAAMSS and PU/PAAM/SS

Sample code	NCO/OH Ratio	PU (mole %)	Starch content (weight %)	PAMM (mole %)	Ultimate tensile strength (Kg/cm^2)		% Elongation at break	
					Dry state	Swollen state	Dry state	Swollen state
PAAM	-	-	-	100	1.2	3.3	60	140
PAAMSS	-	-	2	100	3.8	5.9	80	170
PU/PAAM	2.5	20	-	80	15	11	240	280
PU/PAAM/SS	2.5	20	2	80	19	14	320	380

3.7. Morphology

Scanning electron micrographs of pure sago starch, PAAM, PAAMSS and PU/PAAM/SS networks are shown in Figure 4. The surface morphology of all networks showed a porous structure with voids in between. SEM images of the PAAM network showed crosslinked structures with disrupted surfaces. The finish looks more continuous rather than choppy. Since the structure is crosslinked and has hydrophilic groups except for the side parts, high water absorption can be expected.

SEM images of pure starch showed a globule like structure. It can be clearly seen that the sago starch consists of smooth surfaces and oval or egg-shaped granules. SEM images of PAAMSS looks like fracture surfaces. The change of shape for sago starch from round and smooth to sharp-edged in PAAMSS is because of sago starch chain penetration with acrylamide monomer. Significant morphological differences between different networks confirmed the grafting of starch into the PAAM network. These studies show that incorporating starch concentration results in a tougher material due to chain penetration.

SEM images of PU/PAAM/SS biocomposites showed rough surfaces with dispersed polyacrylamide and starch particles. The structure of the biocomposite was completely different from the PAMM structure, clearly indicating that the interpenetration of acrylamide and starch occurred on the polyurethane network. The rough surface is clearly due to monomer mixing, indicating entanglements and interactions between the polyurethane and the starch and acrylamide networks. Similarly, the incorporation of starch into polyurethane-acrylamide networks worked. This is because starch incorporation provides compatibility within the network. Therefore, the starch-grafted biocomposite exhibits a well-tolerated structure.

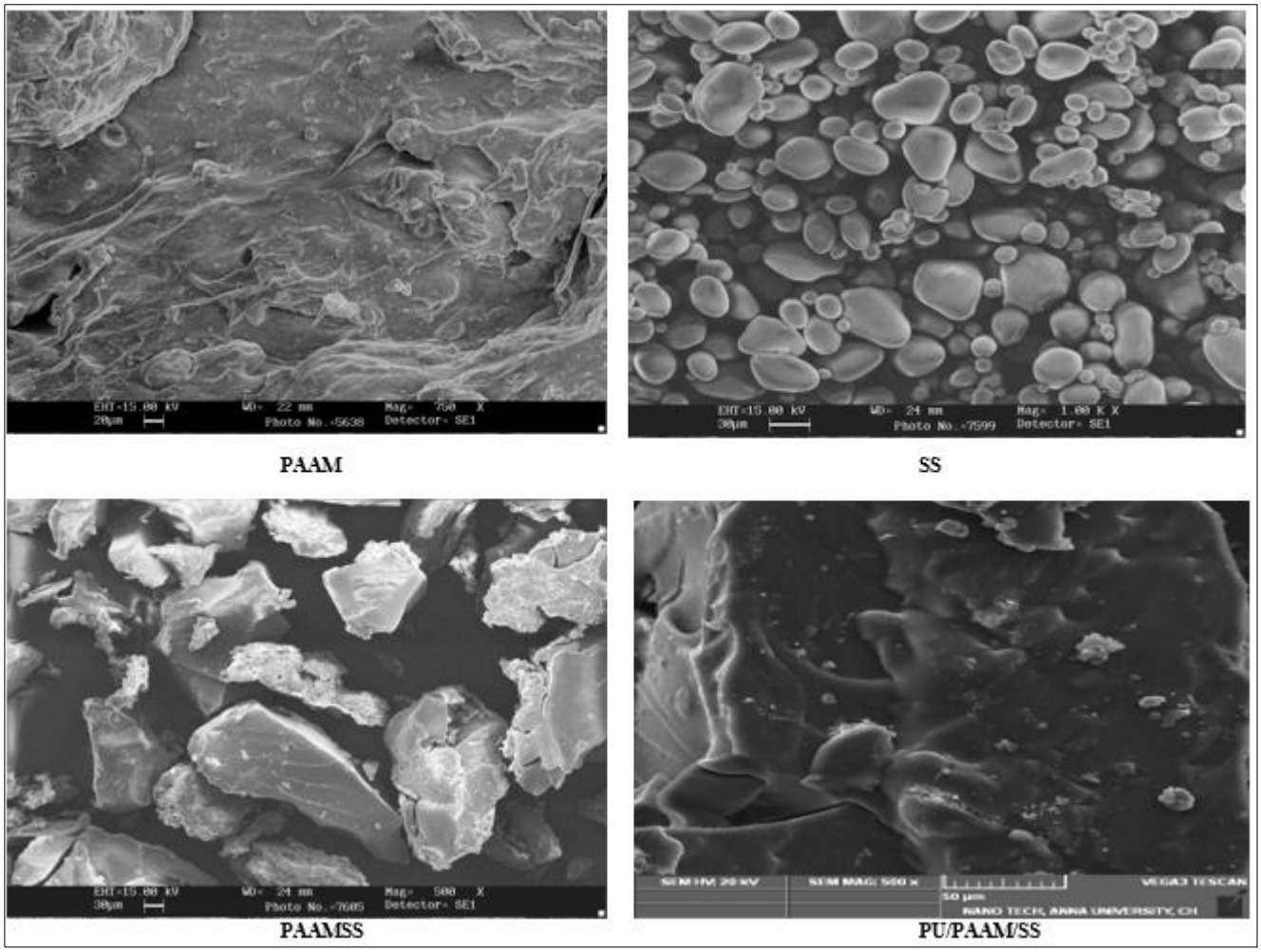

Figure 4. SEM images of a Sample PAAM (a), Pure sago starch (b), PAAMSS (c), and PU/PAAM/SS (e). The interactions between PU, AAM and SS contents are evidenced from the images shown

3.8. Biodegradation Studies

Biodegradation of polymers involves the following steps:(i) microorganisms that adhere to the polymer surface, (ii) microorganisms that grow on the carbon source provided by the polymer, and (iii) primary polymer degradation followed by final degradation. The main degradation of polymers was catalyzed by enzymes and free radicals secreted by microorganisms. This causes depolymerization by cleaving the backbone into oligomers, dimers and monomers. Hydrophilic and water-absorbing polymers are susceptible to microbial attack and have easy water-mediated access to the interior of the matrix [36].

Soil Burial Degradation Study

Figure 5 shows the variation in mass loss (%) of all samples after recovery at regular intervals of 7, 14, 21, and 28 days for soil burial studies. Investigations (Table 5) show that the samples initially show only a slight increase in mass loss due to decomposition. The mass loss of PAAM, PAAMSS, PU/PAAM, and PU/PAAM/SS biocomposite samples was significant after 7 days. This is due to the hydrophilicity of the samples as they contain CONH2 or OH functional groups from hydrolyzed sago starch. Degradation is initiated by the uptake of water from the soil, allowing microorganisms to attack readily susceptible bonds present in the sample. Thus, the resulting biocomposites had improved biodegradability due to the incorporation of sago starch into the network [37].

Table 5. Mass loss data for PAAM, PAAMSS and PU/PAAM/SS

Sample code	% Mass loss by soil burial degradation			
	Days			
	7	14	21	28
PAAM	0.5	1.64	2.73	3.12
PAAMSS	0.59	1.74	2.82	3.20
PU/PAAM	0.51	1.49	2.34	3.35
PU/PAAM/SS	0.53	1.58	2.61	3.71

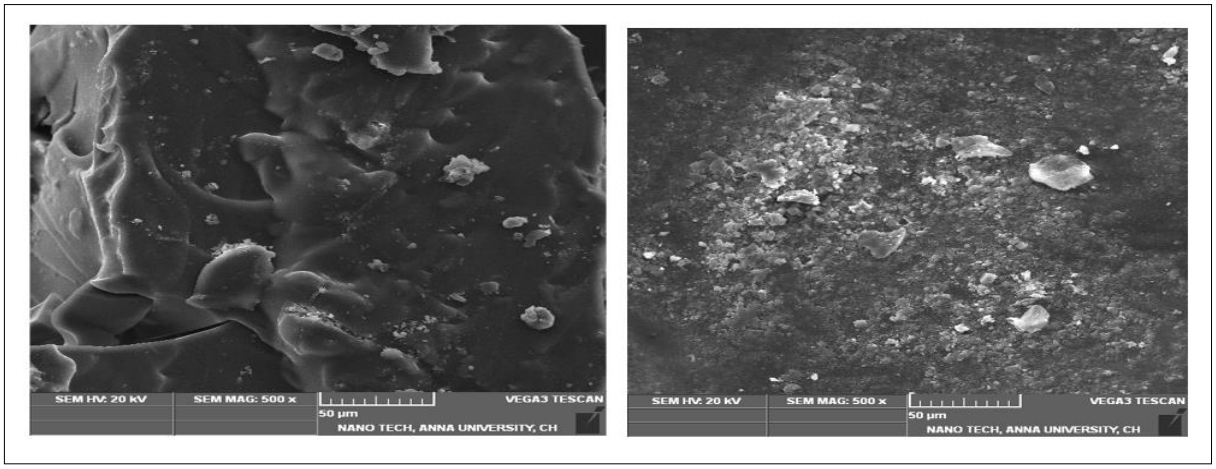

Figure 5. SEM image of PU/PAAM/SS sample before and after degradation (28 days). The degradation of the biocomposite confirmed from the image shown

4. Conclusions

A biocomposite sample made from NCO-terminated polyurethane prepolymer, acrylamide monomer and sago starch were successfully developed by grafting technique. The resulting biocomposite samples exhibited superior thermal stability, conformability, tensile and elongation properties compared to single polyacrylamide networks. The presence of polyurethane in biocomposite samples indicated the flexibility of the samples compared to pure polyacrylamide networks. FTIR spectroscopy results confirmed the grafting of NCO-terminated polyurethane prepolymer, acrylamide monomer and sago starch. Morphological examination using SEM technique showed the suitability of the biocomposite film. The swelling properties of the biocomposite samples were enhanced by the incorporation of sago starch but decreased by the presence of the polyurethane prepolymer. At acidic *p*H, the swelling properties of biocomposites decreased, and at basic *p*H, the opposite trend was observed. The biocomposite was found to be hydrolytically stable in phosphate buffer solution. Sample degradation was demonstrated by soil burial studies. Biodegradation of the biocomposite samples was confirmed by percent mass loss. From this, we can conclude that the developed biodegradable bicomposite materials are promising candidates for potential applications in biomaterials and eco-friendly packaging systems.

References

1. LI MC, GE X, CHO UR., Emulsion Grafting Vinyl Monomers onto Starch for Reinforcement of Styrene-Butadiene Rubber. Macromol. Res 2013; 21(5): 519-28.
2. LI MC, GE X, CHO UR., Mechanical Performance, Water Absorption Behavior and Biodegradability of Poly (methyl methacrylate)-Modified Starch/SBR Biocomposites. Macromol. Res 2013; 21(7): 793-100.
3.PETRINI P, FARE S, PIYA A, TANZI MC., Design, synthesis and properties of polyurethane Hydrogels for tissue engineering J Mater Sci Mater Med 2003; 14(8): 683-86.
4.DROR M, ELISABER MZ, BERRY GC., Gradient interpenetrating polymer networks. I. Poly (ether urethane) and polyacrylamide IPN.J Appl Polym Sci 1981; 26(6):1741-57.

5.FANGXING LI, JU ZUO, LIMER DONG, WANG HJ., Study on the synthesis of high elongation polyurethane Eur Polym J 1998; 34(1): 59-66.
6.SHAN-YANG LIN, KO-SHAO CHEN, LIANG RUN-CHU, Design and evaluation of drug loaded wound dressing having thermoresponsive, adhesive, absorptive and easy peeling properties. Biomaterials 2001;22: 2999–3004.
7.NEVISSAS V, WIDMAIER JM, MEYER GC., Effect of crosslink density and internetwork grafting on the transparency of polyurethane/polystyrene interpenetrating polymer networks. J Appl Polym Sci1988; 36: 1467–73.
8.KIM SJ, KIM SI., Thermal characterization of chitosan and polyacrylamide semi-interpenetrating polymer networks. High Perform Polym 2002; 14: 309-16.
9.MUNIZ EC, GEUSKENS G., Polyacrylamide hydrogels and semi-IPNs with poly (N-isopropyl-acrylamide): mechanical properties by measure of compressive elastic modulus. J Mater Sci Mater Med2001; 12: 879–81.
10.CLAYTON AB, CHIRILA TV, LOU X., Hydrophilic sponges based on 2-Hydroxyethyl metha-crylate.V. Effect of crosslinking agent reactivity on mechanical properties. Polymer International. 1997; 44**:** 201-07.
11.MONLEÓN-PRADAS M, GÓMEZ-RIBELLES JL, SERRANO-AROCA Á, GALLEGO FERRER G, SUAY ANTÓN J, PISSIS P. Porous poly (2-hydroxyethyl acrylate) hydrogels. Polymer2001; 42(10):4667-74.
12.AHMED EM., Hydrogel: Preparation, characterization, and applications: A review. Journal of Advanced Research. 2015; 6(2):105-21.
13.TANAKA T., Gels Scientific American. 1981; 244(1):124-36.
14.YONG QIU, KINAM PARK, Superporous IPN hydrogels having enhanced mechanical properties. AAPS PharmSciTech 2003; 4: 406-12.
15.PRABHA NAIR D, JABALAN M., Polyurethane -polyacrylamide IPNs. I. synthesis and characterization. J Polym Sci a Polym Chem 1990; 28: 3775-86.
16.KIING SC, DZULKEFLY K, YIU PH., Characterization of Biodegradable Polymer Blends of Acetylated and HydroxypropylatedSago Starch and Natural Rubber. J Polym Environ 2013; 21(10): 995-1001.
17.BEG MDH, KORMIN S, BIJARIMI M, ZAMAN HU., Preparation and Characterization of Low-Density Polyethylene/Thermoplastic Starch Composites. Adv. Polym. Technol 2016; 35(1): 21521-9.
18.PRACHAYAWARAKORN J, SANGNITIDEJ P, BOONPASITH P., Properties of thermoplastic rice starch composites reinforced by cotton fiber or low-density polyethylene. Carbohydr. Polym 2010; 81(2): 425-33.
19.YOUSSEF AM, GENDY AE, KAMEL S., Evaluation of corn husk fibers reinforced recycled low density polyethylene composites. Mater. Chem.Phys 2015; 152(1): 26-33.
20.KIM CH, CHO KY, PARK JK., Grafting of glycidyl methacrylate onto polycaprolactone: preparation and characterization. Polymer, 2001; 42(12):5135-42.
21.ZHANG YU, YAMEI L, ZHU M, FANB, YAN R, WU Q., Starches modified with polyurethane micro-particles: Effects of hydroxyl numbers of polyols in polyurethane Carbohydr.Polym 2012; 88(4): 1208-13.
22.TANRATTANAKUL V, PANWIRIYARAT W., Compatibilization of low-densitypolyethylene/ cassava starch blends by potassium persulfate and benzoyl peroxide. J. Appl. Polym. Sci. 2009;114(2): 742-53.
23.MANJUNATH L, SAILAJA RRN, Starch/polyethylene nanocomposites: Mechanical, thermal, and bio-degradability characteristics. Polym. Compos 2016; 37(5): 1384-95.
24.KRISTO E, BILIADERIS CG., Physical properties of starch nanocrystal-reinforced pullulan films. Carbohydr. Polym 2007; 68(1): 146-58.
25.YANG W, KENNY JM, PUGLIA D., Structure and properties of biodegradable wheat gluten bionano-composites containing lignin nanoparticles. Ind. Crops Prod 2015; 74(1): 348-56.

26.LI MC, WU Q, SONG K, CHENG HN, SUZUKI S, LEI T., Chitin Nanofibers as Reinforcing and Antimicrobial Agents in Carboxymethyl Cellulose Films: Influence of Partial Deacetylation.ACS Sustain. Chem. Eng. 2016; 4 (8): 4385-95.
27.TUNCER C, ILKAY A., Synthesis and network structure of ionic poly*(N,N*-Dimethylacrylamide-co-acrylamide) hydrogels: Comparison of swelling degree with Theory. Eur Polym J 2006; 42(6): 1437-45.
28.SEN M, GUVEN O., Prediction of swelling behaviour of hydrogels containing diprotic acid moieties. Polymer 1998; 39(5): 1165-72.
29.YOU Z, KUI-CHUN W, YA-XIN G, YUN- XUE L, JIN-BO Z., Effect of elastic polyurethane on swelling/ deswelling behaviour of polyacrylamide hydrogels. Ziran Kexueban 2004; 20(1): 192-5.
30.GOMEZ ANTON MR, RODRIGUEZ JG, PIEROTA IF., Polymer Effects in Proton-Transfer Reactions. Poly (2-vinylquinoline). Macromolecule 1986; 19(12): 2932-36.
31.KASMA S, KUMAR V, KAITH BS, KUMAR V, SOM S, SUSHEEL K, SWART HC., A study of the biodegradation behaviour of poly(methacrylicacid/aniline) grafted gum ghatti by a soil burial method. Royal Society of Chemistry advance 2014; 4(49): 25637-49.
32.NAYAK BR, SINGH RP., Development of graft copolymer flocculating agents based on hydroxy-propyl guar gum and acrylamide. J. Appl. Polym. Sci., 2001; 81(7): 1776-85.
33. KOEINING MF, HUANG SJ., Biodegradable blends and composites of polycaprolactone and starch derivatives. Polymer 1995; 36(9): 1877-82.
34. LAI YC., Novel polyurethane - silicone hydrogels. J. Appl. Polym. Sci 1995; 56: 301-10.
35.HUANG J, LINA Z., Efects of NCO/OH molar ratio on structure and properties of graft- inter-penetrating polymer networks from polyurethane and nitrolignin. Polymer 2002; 43: 2287-94.
36.LUCAS N, BIENAIME C, BELLOY C, QUENEUDEC M, SILVESTRE F, SAUCEDO JEN, Polymer biodegradation: Mechanisms and estimation techniques - A review. Chemosphere 2008; 73:429-43.
37. SHAMSABADI MA, BEHZAD T, BAGHERI, NASRABADI BN, Preparation and characterization of low-density polyethylene / thermeplastic starch composites reinforced by cellulose nanofibers. Polymer composites 2015; 36:2309-17.

Manuscript received: 20.09.2022